

Optical properties and antimicrobial activity of sol-gel synthesis of $\text{GdMnO}_3\text{-GdMn}_2\text{O}_5$ composite

2

J. Gajendiran¹, S. Gnanam², P. Prameela¹, J. Ramana Ramya³, M. Karthikeyan¹, C. Vinoth¹, S. Gokul Raj⁴, and G. Ramesh Kumar⁵

¹Department of Physics, Vel Tech Rangarajan Dr. Sagunthala R&D Institute of Science and Technology, Chennai, Tamil Nadu, India, ²Department of Physics, School of Basic Sciences, Vels Institute of Science, Technology & Advanced Studies (VISTAS), Chennai, Tamil Nadu, India, ³Department of Periodontics, Saveetha Dental College and Hospitals, Saveetha Institute of Medical and Technical Sciences, Chennai, Tamil Nadu, India, ⁴Department of Physics, Pondicherry University, Puducherry, India, ⁵Department of Science and Humanities, University College of Engineering Arni, Anna University, Chennai, Tamil Nadu, India

2.1 Introduction

There are several pathogenic bacteria, viruses, and fungal diseases that have affected human beings and created a disturbance in the living life of humans. It is a critical and severe problem for public health. Resolving this problem requires some antibiotic resistance-related material from the pharmaceutical and medical industries (Muteeb et al., 2023). It is a challenging task to develop antibiotics with significant effects on the drug industry.

Nanotechnology is an emerging field in science and technology especially in biomedical applications such as antibacterial, antioxidant, and hemolysis for the development of metal oxides (ZnO , CuO , TiO_2 , SnO_2 , NiO , Co_3O_4), metal particles (Ag , Au , Cu), and composite materials at the atomic scale in nano-dimension regimes (Alizadeh et al., 2023; Arun Paul et al., 2023; Dabhane et al., 2021; Isa Khan et al., 2020; Jaffari et al., 2019; Jan et al., 2014; Lavanya et al., 2023; Meena Kumari and Philip, 2015; Nguyen et al., 2023; Pratibha et al., 2024; Selvam et al., 2024; Thakur et al., 2024; Vinotha et al., 2019). The reason for selecting the aforementioned materials is their unique physicochemical properties, good biocompatibility, large surface-to-volume ratio, nontoxicity, etc. In recent years, the aforementioned nanomaterials with various morphologies of nanostructures have been synthesized with promising antibacterial processes, and consequently, they effectively decompose the cells of the microbes through electrostatic force with pathogenic microbes or by penetrating within them, proposing an idea to address the healthcare challenges posed by antibiotic-resistant bacteria.

There are extensive studies on the antibacterial and antioxidant properties of silver nanoparticles, Cu nanoparticles, and semiconductor oxide materials (ZnO, CuO, TiO₂, Ag₂O, Co₃O₄) (Arun Paul et al., 2023; Dabhane et al., 2021; Isa Khan et al., 2020; Jan et al., 2014; Meena Kumari and Philip, 2015; Nguyen et al., 2023; Thakur et al., 2024; Vinotha et al., 2019). Based on the literature reports, size-controlled and morphology-dependent reactive oxygen species (ROS) were developed in the cell walls as a consequence of the tuning of antimicrobial properties. The above-mentioned size and particle morphology parameters can be obtained in nanomaterials through various chemical routes.

Using different chemical routes, ABO₃-type materials (A and B are two different metals, O-oxygen), such as BiFeO₃, LaTiO₃, LaMnO₃, and LaNiO₃, have been attempted for antibacterial and antioxidant applications (Biswas et al., 2017; Jadhav and Khetre, 2020; Prabitha et al., 2023). Among the ABO₃ materials, GdMnO₃-related work on the antibacterial properties has not been attempted to date.

Magnetism behavior at room temperature, electrical transport, and electromagnetic wave properties of gadolinium manganese oxide compounds were divulged by researchers (Chen et al., 2022; Mitra et al., 2017, 2020; Rasras et al., 2021; Romaguera-Barcelay et al., 2014; Samantaray et al., 2013). The above-mentioned properties would apply to magnetic storage and spintronics-based devices (Chen et al., 2020; Wang et al., 2022). In addition, gadolinium manganese oxide compound-based materials were also fabricated by various physicochemical routes (solvothermal/hydrothermal reaction in autoclave, decomposition of metal-hydroxide precipitate, combustion reaction between metal–fuel complex), followed by inspection of their magnetism responses and electro-optics behavior (Gajendiran et al., 2023; Mitra et al., 2017, 2020; Wang et al., 2023). However, the antibacterial activity of the sol-gel synthesis of the GdMnO₃–GdMn₂O₅ composite has not been investigated to date. Antimicrobial activities of the GdMnO₃–GdMn₂O₅ composite against *Staphylococcus aureus* and *Escherichia coli* have been examined. In addition, the optical properties and band gap value of the GdMnO₃–GdMn₂O₅ result are also presented in detail.

2.2 Experimental

In our earlier reports, the preparation of the GdMnO₃–GdMn₂O₅ composite was successfully explained through the sol-gel process (Gajendiran et al., 2023). In our earlier reports, the structural properties (crystalline state and particle size) and dielectric properties of the GdMnO₃–GdMn₂O₅ composite were discussed (Gajendiran et al., 2023). In this proposed work, the above-synthesized composite has been taken for optical spectrum and antimicrobial activity characterization, and its results have been presented in detail.

2.2.1 Antimicrobial activity

The structural properties of nanocomposites were investigated by a Raman spectrophotometer, Model Renisha W/confocal. The optical absorption characteristic and

band gap energy values of the composite were scrutinized with the aid of a UV-visible spectrum tool using the JASCO UV-VIS. Antimicrobial activity experiments of the $\text{GdMnO}_3\text{-GdMn}_2\text{O}_5$ composite were analyzed using the agar diffusion method.

2.2.2 Antibacterial activity

The bactericidal effectiveness of the synthesized nanocomposite was assessed against two different bacterial strains—*E. coli* and *S. aureus*—via the disk diffusion technique. The agar suspension medium was formulated by mixing 38 g of Mueller-Hinton Agar (MHA) and 1 g of nutrient agar in 1 L of triple-deionized water. The mixture was heated to 100°C and then underwent autoclaving for 15 minutes at a pressure of 103 kPa. The 30 mL agar solution was poured into the Petri plates and permitted to solidify. Following this, the Petri plates were subjected to UV light exposure for 30 minutes. An even distribution of a bacterial suspension totaling 300 μL was applied to the agar plate. Subsequently, an 8 mm well was carefully formed in the agar using a well-borer. The samples, dispersed in water at a concentration of 5 mg/mL, were then added to these wells on the agar plates. The plates were incubated at 37°C in an incubator for one day. Subsequently, the diameter of the inhibition zone was manually determined using a ruler and photographed.

2.3 Results and discussion

Room temperature Raman spectrum measurements were carried out for the $\text{GdMnO}_3\text{-GdMn}_2\text{O}_5$ composite, and it recorded the Raman shift range between 0 and 1000 cm^{-1} , as shown in Fig. 2.1. A strong peak was observed at 366, 496, 498, and 618 cm^{-1} . The aforementioned peaks are representative of the coupling between Mn-O and Gd-O stretching vibration modes, respectively (Lu et al., 2009; Priyadarshinee et al., 2023; Wang et al., 2021). In addition, shoulder peaks were noticed at 101, 137, 180, and 281, which are also related to the gadolinium manganese oxide when compared with the reported high-temperature Raman spectra of the $\text{GdMnO}_3\text{-GdMn}_2\text{O}_5$ composite (Lu et al., 2009; Priyadarshinee et al., 2023; Wang et al., 2021).

An optical absorption spectrum study of the composite was recorded in the wavelength range between 300 and 800 nm (Fig. 2.2). The purpose of the above study is to identify the band gap nature of the composite. In addition, how the optical absorption changes with increasing wavelength is also recorded. Optical absorption has been found to increase toward the visible region with increasing wavelength from 300 to 800 nm. Using optical absorption spectrum data of synthesized compounds to determine the band gap energy of this material. Using the optical band gap energy formula ($E_g = hc/\lambda_{\text{abs}}$) and detecting the optical absorption peak at the wavelength of 403 nm, the optical band gap value of the synthesized composite is found to be 3.07 eV. One of these methods will help find the energy gap of the material (Antony and Jagannathan, 2024).

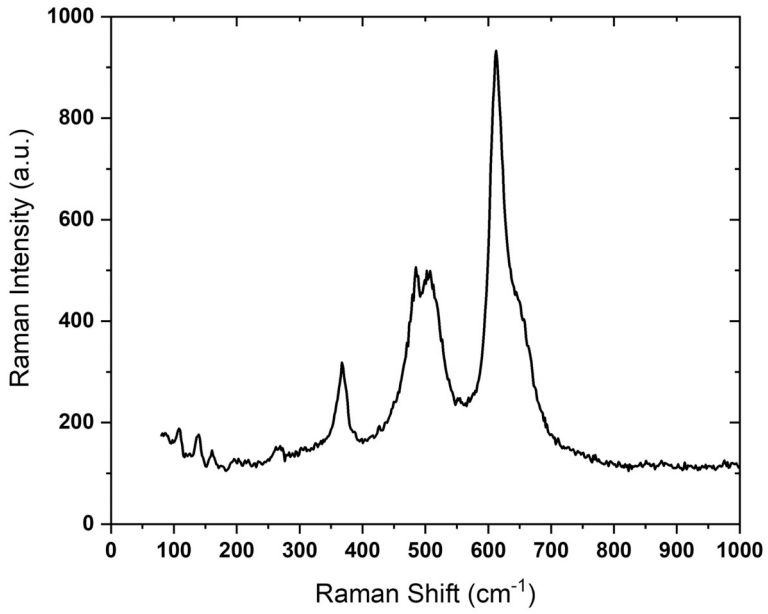


Figure 2.1 Raman spectrum of the GdMnO₃-GdMn₂O₅ composite.

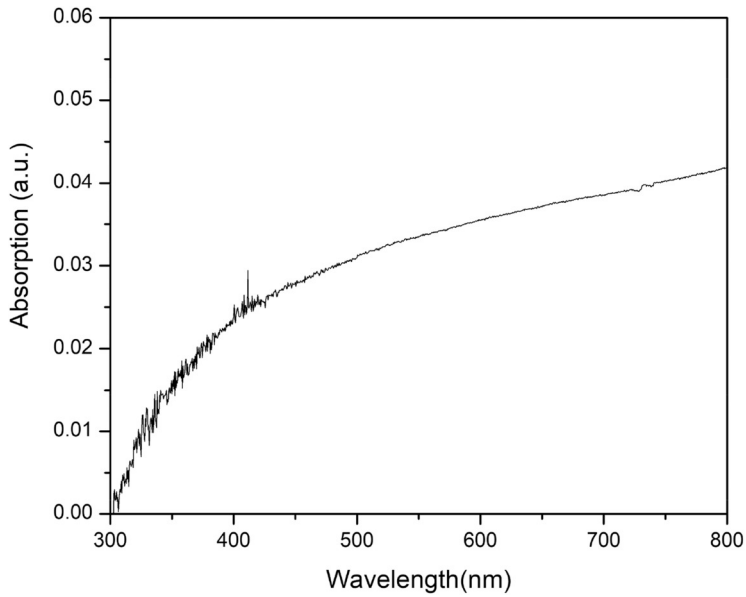


Figure 2.2 UV-visible spectrum of the GdMnO₃-GdMn₂O₅ composite.

The antibacterial efficacy of the $\text{GdMnO}_3\text{-GdMn}_2\text{O}_5$ composite sample was assessed using the well-diffusion technique (Ramya et al., 2024) against *E. coli* and *S. aureus*. The antimicrobial efficacy of the $\text{GdMnO}_3\text{-GdMn}_2\text{O}_5$ composite against *E. coli* and *S. aureus* was determined to be 25 mm and 20 mm, respectively (Fig. 2.3). This suggests that $\text{GdMnO}_3\text{-GdMn}_2\text{O}_5$ exhibits notable antibacterial activity against both bacterial strains (*E. coli* and *S. aureus*). A higher zone inhibition width has been found for the *E. coli* bacterial strain than for *S. aureus*. Generally, higher zone inhibition leads to higher microbial responses. The size of the zone of inhibition was varied under the influence of Gram-positive and negative bacterial strains, preparation route, processing condition, and concentration quantity of nanomaterials.

One possible mechanism underlying this efficacy could be ascribed to the liberation of transition metal ions, such as manganese and gadolinium, from the $\text{GdMnO}_3\text{-GdMn}_2\text{O}_5$ composite upon contact with bacterial cells. These metal ions can disrupt essential cellular processes, such as enzyme activity and membrane integrity, leading to bacterial cell death. These nanoparticles interfere with enzyme activity, leading to the inhibition of vital metabolic pathways. The metal ions can generate oxidative stress by creating reactive oxygen species (ROS) within the bacterial cell wall. ROS can break the cellular components such as DNA, proteins, and lipids, ultimately leading to cell death. Moreover, the nanoparticles' high surface area allows for increased interaction with the bacterial cell membrane, potentially disrupting cellular integrity and consequently causing outflow of cellular contents. Also, bacterial cell death induced by nanocomposites can occur through various mechanisms involving interactions with biomolecules like amino acids, thiols, and imidazole groups present in bacterial cells. Nanoparticles may disrupt essential cellular functions by binding to amino acids, interfering with protein synthesis and enzyme activity crucial for bacterial survival. Thiols, found in proteins and enzymes, are susceptible to oxidation by nanoparticles, leading to protein dysfunction and cell

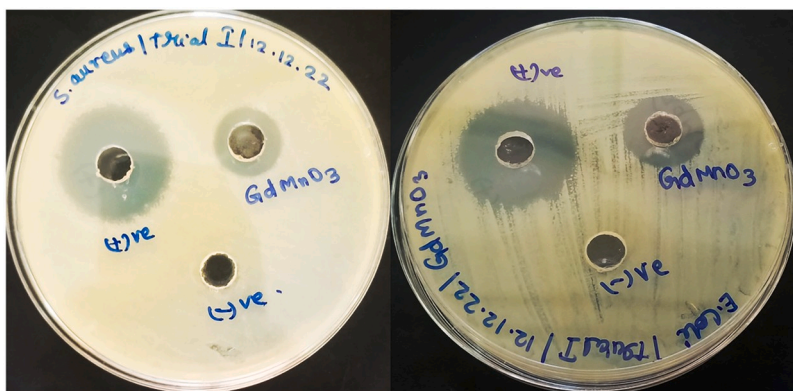


Figure 2.3 Antimicrobial activity of the $\text{GdMnO}_3\text{-GdMn}_2\text{O}_5$ composite against *Staphylococcus aureus* and *Escherichia coli*.

death. The synthesized particles can interact with imidazole groups present in important cellular structures like enzymes and nucleic acids, disrupting their functions and causing cellular damage. Additionally, the high surface area of the $\text{GdMnO}_3\text{-GdMn}_2\text{O}_5$ particles could facilitate increased contact with bacterial cells, enhancing the antimicrobial effect.

2.4 Conclusion

The synthesized composites reveal that coupling between Mn-O and Gd-O stretching vibration modes was confirmed through the Raman spectrum. Using the UV-visible spectrum, the optical absorption was found in the visible region. To investigate the antimicrobial efficiency, the synthesized composite, along with two different bacterial agents, was tested, followed by conducting the disc diffusion method. Using the above method, ZOI values are measured with the help of a scale. Higher zone inhibition values are found for *E. coli* (25 mm) than for *S. aureus* (20 mm). The obtained ZOI values would act as a good antibacterial resistance. Hence, the obtained antimicrobial results of synthesized composites would be a curiosity in biomedical applications.

Acknowledgment

This article is published with the SEED FUND (Ref No: VTU/Seed Fund/FY 2024-2025/017) provided by Vel Tech Rangarajan Dr. Sagunthala R&D Institute of Science and Technology.

References

- Alizadeh, S. R., Seyghalan, H. N., Hashemi, Z., & Ebrahimzadeh, M. A. (2023). *Scrophularia striata* extract mediated the synthesis of gold nanoparticles; their antibacterial, antileishmanial, antioxidant, and photocatalytic activities. *Inorganic Chemistry Communications*, 156, 111138. <https://doi.org/10.1016/j.inoche.2023.111138>.
- Antony, T. J., & Jagannathan, K. (2024). Structural, morphological and optical properties of ZnFe_2O_4 -decorated reduced graphene oxide nanocomposite for antibacterial applications. *Ceramics International*, 50, 16343–16351. <https://doi.org/10.1016/j.ceramint.2024.02.116>.
- Arun Paul, C., Ranjith Kumar, E., Abd El-Rehim, A. F., & Yang, G. (2023). Analysis and characterization of structural, morphological, thermal properties and colloidal stability of CuO nanoparticles for various natural fuels. *Ceramics International*, 49, 31193–31209. <https://doi.org/10.1016/j.ceramint.2023.07.065>.
- Biswas, K., De, D., Bandyopadhyay, J., Dutta, N., Rana, S., Sen, P., Ky, B. S., & Ky, C. P. (2017). Enhanced polarization, magnetic response, and pronounced antibacterial activity of bismuth ferrite nanorods. *Materials Chemistry and Physics*, 195, 207–212. <https://doi.org/10.1016/j.matchemphys.2017.04.020>.
- Chen, J., Dai, H. Y., Wang, M. M., Ye, F. J., Li, T., Xu, M. S., & Chen, Z. P. (2020). An evaluation of the impact of Ca substitution on the structural and magnetic properties of

- GdMnO₃ ceramics. *Ceramics International*, 46, 6360–6367. <https://doi.org/10.1016/j.ceramint.2019.11.112>.
- Chen, J., Zhang, G., Liu, H., Dai, X., Zhao, R., Li, T., & Dai, H. (2022). Evolution of structure, vacancy characteristics, dielectric and magnetic properties of GdMnO₃ ceramics induced by Li⁺ ion substitution. *Journal of Magnetism and Magnetic Materials*, 564, 170156. <https://doi.org/10.1016/j.jmmm.2022.170156>.
- Dabhane, H., Zate, M., Bharsat, R., Jadhav, G., & Medhane, V. (2021). A novel bio-fabrication of ZnO nanoparticles using cow urine and study of their photocatalytic, antibacterial and antioxidant activities. *Inorganic Chemistry Communications*, 134, 108984. <https://doi.org/10.1016/j.inoche.2021.108984>.
- Gajendiran, J., Gnanam, S., Ramachandran, K., Bharath Sabarish, V. C., Durairajan, A., Graça, M. P. F., Valente, M. A., Gokul Raj, S., & Ramesh Kumar, G. (2023). Study of the structural, magnetic and dielectric properties of GdMnO₃-GdMn₂O₅ nanocomposites via sol-gel route. *Materials Letters*, 330, 133311. <https://doi.org/10.1016/j.matlet.2022.133311>.
- Isa Khan, M., Nawaz, M., BilalTahir, M., Iqbal, T., Pervaiz, M., Rafique, M., Aziz, F., Younas, U., & Alrobei, H. (2020). Synthesis, characterization and antibacterial activity of NiO NPs against pathogen. *Inorganic Chemistry Communications*, 122, 108300. <https://doi.org/10.1016/j.inoche.2020.108300>.
- Jadhav, A. L., & Khetre, S. M. (2020). Antibacterial activity of LaNiO₃ prepared by sonicated sol-gel method using combination fuel. *International Nano Letters*, 10, 23–31. <https://doi.org/10.1007/s40089-019-00285-7>.
- Jaffari, Z. H., Lam, S. M., Sin, J. C., & Zeng, H. (2019). Boosting visible light photocatalytic and antibacterial performance by decoration of silver on magnetic spindle-like bismuth ferrite. *Materials Science in Semiconductor Processing*, 101, 103–115. <https://doi.org/10.1016/j.mssp.2019.05.036>.
- Jan, T., Iqbal, J., Ismail, M., Badshah, N., Mansoor, Q., Arshad, A., & Ahkam, Q. M. (2014). Synthesis, physical properties and antibacterial activity of metal oxides nanostructures. *Materials Science in Semiconductor Processing*, 21, 154–160. <https://doi.org/10.1016/j.mssp.2014.01.006>.
- Lavanya, M., Krishnamoorthy, R., Alshuniaber, M. A., Manoharadas, S., Perumal Palanisamy, C., PriyaVeeraraghavan, V., Jayaraman, S., Rajagopal, P., & Padmini, R. (2023). Formulation, characterization and evaluation of gelatin-syringic acid/zinc oxide nanocomposite for its effective anticancer, antioxidant and anti-inflammatory activities. *Journal of King Saud University - Science*, 35, 102909. <https://doi.org/10.1016/j.jksus.2023.102909>.
- Lu, C. L., Fan, J., Liu, H. M., Xia, K., Wang, K. F., Wang, P. W., He, Q. Y., Yu, D. P., & Liu, J. M. (2009). An investigation on magnetism, spin-phonon coupling, and ferroelectricity in multiferroic GdMn₂O₅. *Applied Physics A*, 96, 991–996. <https://doi.org/10.1007/s00339-009-5133-2>.
- Meena Kumari, M., & Philip, D. (2015). Synthesis of biogenic SnO₂ nanoparticles and evaluation of thermal, rheological, antibacterial and antioxidant activities. *Powder Technology*, 270, 312–319. <https://doi.org/10.1016/j.powtec.2014.10.034>.
- Mitra, A., Mahapatra, A. S., Mallick, A., & Chakrabarti, P. K. (2017). Room temperature magnetic ordering, enhanced magnetization and exchange bias of GdMnO₃ nanoparticles in (GdMnO₃)_{0.70}(CoFe₂O₄)_{0.30}. *Journal of Magnetism and Magnetic Materials*, 424, 388–393. <https://doi.org/10.1016/j.jmmm.2016.10.065>.
- Mitra, A., Shaw, A., & Chakrabarti, P. K. (2020). Microstructure, dielectric, ferroelectric and magnetoelectric coupling of a novel multiferroic of [(GdMnO₃)_{0.7}(CoFe₂O₄)_{0.3}]

- 0.5[TiO₂]_{0.5} nanocomposite. *Materials Chemistry and Physics*, 240, 122242. <https://doi.org/10.1016/j.matchemphys.2019.122242>.
- Muteeb, G., Rehman, M. T., Shahwan, M., & Aatif, M. (2023). Origin of antibiotics and antibiotic resistance, and their impacts on drug development: A narrative review. *Pharmaceuticals*, 16(11), 1615. <https://doi.org/10.3390/ph16111615>.
- Nguyen, T. T. T., Nguyen, Y. N. N., Tran, X. T., Nguyen, T. T. T., & Tran, T. V. (2023). Green synthesis of CuO, ZnO and CuO/ZnO nanoparticles using *Annona glabra* leaf extract for antioxidant, antibacterial and photocatalytic activities. *Journal of Environmental Chemical Engineering*, 11, 111003. <https://doi.org/10.1016/j.jece.2023.111003>.
- Prabitha, V. G., Sahadevan, J., Madhavan, M., Muthu, S. E., Kim, I., Sudheer, T. K., & Sivaprakash, P. (2023). Effect of Yttrium doping on antibacterial and antioxidant property of LaTiO₃. *Discover Nano*, 18, 155. <https://doi.org/10.1186/s11671-023-03942-1>.
- Pratibha, Rajoriya, K., Singhal, A., Meena, R., & Kumari, A. (2024). Biogenic synthesis and characterisation of *Flueggea leucopyrus* willd leaf mediated copper nanoparticles for antibacterial, antioxidant, and antidiabetic activities. *Journal of Herbal Medicine*, 44, 100859. <https://doi.org/10.1016/j.hermed.2024.100859>.
- Priyadarshinee, S., Pati, J., Mahapatra, R., Mohanty, P., Mishra, D. K., & Mohapatra, J. (2023). Studies of structural, microstructural, optical and dielectric properties of GdMnO₃. *Journal of the Korean Ceramic Society*, 60, 203–214. <https://doi.org/10.1007/s43207-022-00256-3>.
- Ramya, J. R., Ali, S., ThanigaiArul, K., Vijayalakshmi, R., Gajendiran, J., Gnanam, S., & Ramachandran, K. (2024). Antimicrobial efficiency against fish pathogens on the green synthesized silver nanoparticles. *Microbial Pathogenesis*, 193, 106725. <https://doi.org/10.1016/j.micpath.2024.106725>.
- Rasras, A., Hamdi, R., Mansour, S., Samara, A., & Haik, Y. (2021). Study of the magnetocaloric effect in single-phase antiferromagnetic GdMnO₃. *Journal of Physics and Chemistry of Solids*, 149, 109798. <https://doi.org/10.1016/j.jpcs.2020.109798>.
- Romaguera-Barcelay, Y., Agostinho Moreira, J., Almeida, A., Tavares, P. B., & Pérez de la Cruz, J. (2014). Structural, electrical and magnetic properties of magnetoelectric GdMnO₃ thin films prepared by a sol–gel method. *Thin Solid Films*, 564, 419–425. <https://doi.org/10.1016/j.tsf.2014.06.007>.
- Samantaray, S., Mishra, D. K., Pradhan, S. K., Mishra, P., Sekhar, B. R., Behera, D., Rout, P. P., Das, S. K., Sahu, D. R., & Roul, B. K. (2013). Correlation between structural, electrical and magnetic properties of GdMnO₃ bulk ceramics. *Journal of Magnetism and Magnetic Materials*, 339, 168–174. <https://doi.org/10.1016/j.jmmm.2013.03.015>.
- Selvam, K., Sudhakar, C., & Ragu Prasath, A. (2024). Green synthesis and characterization of silver nanoparticles from sandalwood (*Santalum album* L.) extract for efficient catalytic reduction, antioxidant and antibacterial activity. *Biocatalysis and Agricultural Biotechnology*, 57, 103094. <https://doi.org/10.1016/j.bcab.2024.103094>.
- Thakur, N., Thakur, N., Kumar, A., Kumar Thakur, V., Kalia, S., Arya, V., Kumar, A., Kumar, S., & Kyzas, G. Z. (2024). A critical review on the recent trends of photocatalytic, antibacterial, antioxidant and nanohybrid applications of anatase and rutile TiO₂ nanoparticles. *Science of The Total Environment*, 914, 169815. <https://doi.org/10.1016/j.scitotenv.2023.169815>.
- Vinotha, V., Iswarya, A., Thaya, R., Govindarajan, M., Alharbi, N. S., Kadaikunnan, S., Khaled, J. M., Al Anbr, M. N., & Vaseeharan, B. (2019). Synthesis of ZnO nanoparticles using insulin-rich leaf extract: Anti-diabetic, antibiofilm and anti-oxidant properties.

- Journal of Photochemistry and Photobiology B: Biology*, 197, 111541. <https://doi.org/10.1016/j.jphotobiol.2019.111541>.
- Wang, M., Dai, H., Li, T., Chen, J., Yan, F., Xue, R., Xing, X., Chen, D., Ping, T., & He, J. (2021). The evolution of structure and properties in $\text{GdMn}_{(1-x)}\text{Ti}_x\text{O}_3$ ceramics. *Journal of Material Science Material Electronics*, 32, 27348–27361. <https://doi.org/10.1007/s10854-021-07106-8>.
- Wang, M., Wang, R., Dai, H., Li, T., Sun, Y., Liu, D., Yan, F., & Xing, X. (2022). The effects of hot isostatic pressing temperature on the structure and properties in GdMnO_3 ceramics. *Ceramics International*, 48, 3685–3694. <https://doi.org/10.1016/j.ceramint.2021.10.150>.
- Wang, N., You, K. Y., Mohanavel, V., Mehrez, S., Alamri, S., Nag, K., & Mahariq, I. (2023). Comprehensive study of electromagnetic wave absorption properties of GdMnO_3 - MoSe_2 hybrid composites. *Ceramics International*, 49, 9191–9202. <https://doi.org/10.1016/j.ceramint.2022.11.082>.